BNL-101512-2014-TECH

AD/AP 22;BNL-101512-2013-IR

# The BNL Heavy-Ion Beam Facility

A. G. Ruggiero

January 1991

Collider Accelerator Department

**Brookhaven National Laboratory**

**U.S. Department of Energy**

USDOE Office of Science (SC)

# DISCLAIMER

AD/AP-22

Accelerator Development Department
Accelerator Physics Division
BROOKHAVEN NATIONAL LABORATORY
Associated Universities, Inc.
Upton, NY 11973

**Accelerator Physics Technical Note No. 22**

# The BNL Heavy–Ion Beam Facility

A.G. Ruggiero

January 1991

# The BNL Heavy-Ion Beam Facility

A.G. Ruggiero
Accelerator Development Department
January 1991

Submitted to U.S. Particle Accelerator School, BNL, Upton, New York, July 24 - August 4, 1989.

# The BNL Heavy–Ion Beam Facility*

A.G. Ruggiero

Brookhaven National Laboratory
Upton, NY 11973, USA

## Introduction

Brookhaven National Laboratory (BNL) has a unique facility made of several accelerators linked together to provide beams of heavy ions with different charge state, atomic mass, intensity and energy. Of course, there are other examples of accelerators clustered together where beams of one type of particles are accelerated or stored in different stages. The Tevatron complex at Fermilab is one example for protons and antiprotons. Another example is LEP, the electron–positron collider in CERN, with the multi–ring system that makes up the source. Indeed it has become rather ingenuous to find ways of using existing accelerators for new and more advanced applications, for instance accelerating different types of particles, or even converting older accelerators into storage rings and eventually colliders. In all these cases the required beams are generated in one corner of the laboratory, accelerated, transferred and manipulated in a variety of ways through several components and finally used in a collider. This method has also been found to be economical, since several parts do not have to be build from anew.

We shall describe here the heavy ion complex at BNL. It is made of the following parts:

- the TANDEM, that is the heavy ion source proper,
- the Heavy Ion Transfer Line (HITL), which takes the beams of heavy ions to the AGS or the Booster,
- the AGS Booster, where the ions are accelerated to an energy large enough to achieve full stripping,
- the AGS, where fully stripped ions are accelerated to an energy in excess of 10 GeV/nucleon
- the transfer lines from the AGS to RHIC, and

* Work performed under the auspices of the U.S. Department of Energy.

• the Relativistic Heavy Ion Collider (RHIC), the final stage of the BNL complex.

A view of the BNL site with the relative location of the components of the Heavy Ion Facility is given in Figs. 1 and 2.

## The TANDEM Accelerator

The TANDEM accelerator is an electrostatic machine that works on an old, but still very effective, principle which was first proposed by R. J. Van de Graaff in 1931. The principle is schematically shown in Figs. 3 and 4. A high voltage is generated on a terminal by making use of the convective currents carried by a belt charged up by another lower voltage electrostatic generator. In the example of the BNL accelerator the terminal can be set at the voltage of 15 MVolt. The source of ions is located near ground where it can be easily reached for replacement and maintenance. The beam is initially stripped of one or two electrons and accelerated by $\sim$ 25 keV through a region of high pressure gas made of a chemical element (Cesium) that easily releases electrons to the ions to charge them to a -1, thus negative charge state. This process is called "spattering". The negative ions are then accelerated toward the positive high–voltage terminal travelling along the axis of a drift tube penetrating the terminal itself.

Once the high–voltage terminal has been reached, the beam of ions traverses a target thick enough to provide an initial stripping to the desired positive charge state. The target is made of gas for the light ions and can be made of solid material, like carbon, for heavier elements. The target is entirely located in the high–voltage terminal and stripping occurs here. The ions are then accelerated again from the positive voltage down to ground travelling along the second stage of the drift tube. At this point the beam is carried to some distance where, if required, it can cross a second stripping target to obtain a larger charge state.

At the end of acceleration, the final kinetic energy is $(1 + QT) \times 15$ MeV, where QT is the charge state after the first stripping at the terminal. For nuclear and high–energy physics applications, it is more convenient to define the energy per nucleon by dividing the total kinetic energy by the atomic mass number A. The Tandem has very good stability of the high–voltage, better than one part in ten thousand, and the beam accelerated is expected to have a very small energy spread.

The stripping target, which is required to remove the desired number of electrons or, eventually, to fully strip ions of light mass, may also cause some negative side effects. The thickness has to be adjusted to reach the wanted charge state for the given available energy; the higher the energy and easier it will be to remove electrons. For a given thickness there is an energy loss accompanied by a transverse angular spreading and by a spreading of the energy distribution. Despite all this, the resulting momentum spread is better than 0.1% and the rms emittance does not exceed 1 $\pi$-mm-mrad in each transverse plane, also with two stripping targets, the second of them located after the Tandem. A more serious effect is that there is a wide distribution of charge states in exit of a target and, by selecting only the required one, one looses a considerable amount of beam. If the target thickness is properly chosen for the required charge, survival rates of 10-20% have been demonstrated.

The standard mode of operation of a Tandem is to accelerate continuous (dc) beams of ions, as required by the experimental program of low–energy atomic and nuclear physics. Typical currents in output are around one particle–$\mu$A. The limitation is caused by either the available negative ion sources or by the beam loading of the high–voltage terminal. Indeed, as charged particles are accelerated by the terminal they have tendency to lower the potential by an amount proportional to the total charge being accelerated. The voltage drop is compensated by the recharging of the van de Graaff generator which nevertheless has a limited rate. A maximum current is then obtained when the two rates equal each other.

As an injector to circular machine like the Booster, the Tandem is operated more conveniently in a pulsed mode, providing beam in burst of short duration just enough for filling of the subsequent accelerator. The bursts will repeat in succession to match the repetition rate of the Booster and with much larger instant current. This mode of operation has been demonstrated here at BNL. A summary of cases which are taken as examples for the experimental programs of the BNL heavy–ion facility is given in Table 1. In this table we give the charge state QT after the stripping target at the terminal, the survival rate or stripping efficiency ST, the kinetic energy in exit, the relativistic velocity factor $\beta$ and the number of ions per pulse assuming a pulse duration of 110 $\mu$s and a 200 particle- -$\mu$A for the source current. The overall transmission through the two stages of the Tandem is 75 percent. Acceleration of ion species of Gold (Au) has been demonstrated according to the requirements for the RHIC program. Acceleration of Oxygen and Silicon also has been demonstrated though at somewhat lower performance than required for RHIC, but in sufficient amount for the experimental program of the AGS. The case of Uranium is feasible but it requires developing a high–intensity source.

**Table 1:** Tandem Operation Parameters

| | A | QT | ST | Kin. Energy MeV/u | $\beta$ | Ions/Pulse |
|---|---|---|---|---|---|---|
| Deuterium | 2 | +1 | 70% | 15.0 | 0.177 | $7.2 \times 10^{10}$ |
| Oxygen | 16 | +6 | 39 | 6.56 | 0.118 | 4.0 |
| Silicon | 28 | +9 | 30 | 5.36 | 0.107 | 3.1 |
| Copper | 63 | +11 | 27 | 2.86 | 0.078 | 2.8 |
| Iodine | 127 | +13 | 20 | 1.65 | 0.059 | 2.1 |
| Gold | 197 | +14 | 12 | 1.07 | 0.048 | 1.2 |
| Uranium | 239 | +35 | 3.4 | 0.09 | 0.043 | 0.4 |

There are two Tandems at BNL (MP6 and MP7) which can be conveniently used in alternate mode, as shown in Fig. 5.

## The Heavy–Ion Transfer Line (HITL)

The transfer line which takes the beam of heavy ions from the Tandem to the AGS is of recent construction and it was commissioned in 1987. Since the beam is extracted from the Tandem in the direction opposite to the AGS, the line starts first with a sharp 180 degrees bend achieved with two dipoles. Between these two magnets a second stripping target is located to increase, if required, the charge state of the ions. Other major bending exists at the end of the line just prior to the injection to the AGS. Focussing of the beam in the directions transverse to the main motion is done with quadrupoles arranged in a sequence of doublets at roughly 80 meters apart. This insures the beam envelop has waists in the proximity of the quadrupoles in both horizontal and vertical plane. The line is achromatic, that is the particle motion in the long section between bendings does not depend on the particle momentum to first order. An important requirement in the design of the line is matching of the lattice functions with those of the AGS at the injection point. This is required to avoid a mismatch between the focussing properties of the two parts which may cause an oscillatory and pulsating motion of the beam, and eventually a beam size enlargement and loss. At the beginning of the line, the initial values of the lattice functions are taken to match the beam dimensions and aspect ratios in the two 2–dimensional transverse phase planes ($x, x'$ and $y, y'$).

A continuation of the HITL toward the Booster has already been authorized and construction is under progress; when the line will be completed the total length will reach about 800 meter. At the moment only ions of Oxygen and Silicon are transferred fully stripped to the AGS where they are accelerated to about 15 GeV/nucleon and used in a variety of experiments. The present vacuum in the AGS ($10^{-7}$ torr) is adequate for these species. In the near future, after the completion of the Booster, the HITL will take beam of heavier species (like Gold, Au 197) partially stripped to the Booster where it can be accelerated to energies large enough so it can subsequently stripped on the way to the AGS of all the remaining electrons without excessive beam losses and deteriorations. The concepts for the design of the second section of the HITL, which runs outside the AGS tunnel, are the same to those used for the first one.

## The Booster

The AGS Booster is a circular accelerator with the main function of accelerating intense beams of protons to 1.5 GeV at the repetition rate of 7.5 pulses per second and 1.5 $10^{13}$ protons divided in three bunches per pulse. For this purpose the ring circumference has been chosen to be one fourth of that of the AGS so that four beam pulses can be injected in a box car fashion for further acceleration in the AGS.

An equally important function is the acceleration of very heavy ions, like gold (Au), to specific energies of several hundred of MeV/u where the ions can be fully stripped before they are injected into the AGS. The Booster project is at the moment under construction and will be ready for commissioning and operation during 1991.

The Booster is an example of a fast cycling synchrotron; the shape of the ring is shown in Fig. 6. It works on the principle of separated functions, where the action of bending the beam on a circular path is provided by pure dipole field magnets, separated from the function of focussing the motion in both horizontal and vertical direction which is provided by the quadrupole magnets. A list of the main parameters of the Booster is given in Table 2. The design of the ring is based on the alternating gradient principal where the basic element of the magnet lattice is a FODO cell; this gives the effect of strong focussing yielding relatively small transverse dimensions of the beam and henceforth less demanding magnetic aperture. Fig. 7 displays the lattice amplitude functions and the dispersion of one of the eight superperiods which make the accelerator. A superperiod is obtained very simply by three consecutive FODO cells where dipole magnets are removed

**Table 2:** Booster Parameters

| | | | |
|---|---|---|---|
| Circumference | | 201.78 m | |
| No. of periods | | 8 | |
| No. of FODO Cells | | 24 | |
| $\nu_x$ | | 4.82 | |
| $\nu_y$ | | 4.83 | |
| Quadrupoles | QF | 0.281199 $m^{-1}$ | 0.5 m |
| | QD | 0.289866 $m^{-1}$ | 0.5 m |
| Dipoles | | $2\pi/36$ rad | 2.4 m |
| Bending Radius | $\rho$ | 18.75099 m | |
| Transition Energy | $\gamma_t$ | 4.88 | |
| Tuning Range | | $\pm 1$ | |
| Phase Advance/Cell | | $72^o$ | |
| Max. Betatron Func. | $\beta_x$ | 13.87 m | |
| | $\beta_y$ | 13.64 m | |
| | $X_p$ | 2.95 m | |
| Natural Chromaticity | $\xi_x$ | -5.093 | |
| | $\xi_y$ | -5.447 | |

to provide space for beam injection and extraction magnets as well as rf cavities for the beam acceleration.

Acceleration of heavy ions occurs at slower rate, that is one pulse every second. The limit is set by the higher magnetic rigidity that is to be reached and by the maximum variation of the bending field per unit of time set to 8 Tesla/s to control the amount and the effects of the eddy current in the metallic vacuum chamber.

At injection, the beam of heavy ions is a continuous pulse lasting a hundred microseconds or more. Several turns are injected, using a betatron stacking technique by which subsequent beam pulses are placed next to each other in the phase space until the whole available aperture is filled. It is estimated that in the case of Au ions more than 20 turns can be injected. Eventually there is a limit on the maximum intensity that can be reached during injection, which is due to the depression of the betatron tunes due to space charge. This is estimated according to the following formula

$$\Delta\nu \simeq \frac{N r_0 Q^2}{2\beta\gamma^2 B A \epsilon_N}$$

where $N$ is total number of ions injected, $A$ the mass number, $Q$ the charge state, $r_0$ the classical radius of a proton, $B$ the bunching factor defined as the ratio of the average beam current to the peak current after rf capture and bunching, and $\beta$ and $\gamma$ are the usual relativistic factors. Finally $\epsilon_N$ is the so–called normalized emittance, an invariant which measures the phase area occupied by the beam. Table 3 gives a summary of the beam parameters; as one can see, the space–charge limit is not reached in all cases and source development for an intensity increase is useful.

Also the intensity of the proton beam is limited by space–charge. The injection of protons though proceeds in a different manner and it is based on the principle of charge exchange which allows stacking of many pulses essentially on top of each other without violating Liouville's theorem. Instead of protons which are charged positively, negative ions $H^-$ are injected which, once in the ring, are immediately stripped of the two electrons by traversing a thin foil.

In most of the cases, especially for the heavy ones, the ions are injected in the Booster only partially stripped. This causes some concern about particle losses due the capture or loss of electrons by scattering with the atoms and molecules of the residual gas in the vacuum chamber. To reduce the losses to a very small fraction, the vacuum is to be kept to better than $10^{-10}$ mmHg.

Acceleration in the Booster, like any other synchrotron, is based on the principle of stability of phase. Particles are accelerated by the longitudinal electric field in a system of rf cavities which are excited at a frequency which is exactly an integer times the revolution frequency of the beam. In the case of the Booster, the integer, called also the harmonic number, is h=3, so that three beam bunches are formed during the rf capture. The major problem for the design of the rf system is the large frequency range required during the acceleration cycle. Indeed, for instance, for the case of Au–ions, the initial velocity, at injection is $\beta = 0.05$ whereas at he end of the acceleration cycle $\beta = 0.8$. To provide for the frequency swing rf cavities are loaded with ferrite. Table 3 also provides a summary of the rf requirement for acceleration of heavy ions in the Booster.

At the end of the acceleration, the beam is extracted in one single turn and transferred to the AGS. Before, though, it will pass through one more foil to obtain complete stripping if this is required. A short transport line, matched to the two circular accelerators at both ends, takes the beam to the AGS.

**Table 3:** Number of Heavy Ions per Bunch in the Booster

| Species | d | $^{16}O$ | $^{28}Si$ | $^{63}Cu$ | $^{127}I$ | $^{197}Au$ | $^{238}U$ | Units |
|---|---|---|---|---|---|---|---|---|
| Harmonic, $h$ | 1 | 2 | 2 | 2 | 3 | 3 | 3 | |
| $f_{rf}$ @ injection | 262 | 350 | 318 | 232 | 264 | 213 | 190 | kHz |
| $f_{rf}$ @ top energy | 1.40 | 2.68 | 2.60 | 2.08 | 2.23 | 1.66 | 2.85 | MHz |
| Top kinetic energy | 1857 | 1249 | 998 | 376 | 144 | 72 | 279 | MeV/u |
| Ions/Bunch @ S.C. Limit | 807 | 38 | 24 | 19 | 11 | 10 | 11.5 | $\times 10^9$ |
| Ions/Bunch† | 199 | 8.32 | 7.06 | 8.7 | 5.64 | 4.12 | 1.2‡ | $\times 10^9$ |
| Normalized Emittance | 8.8 | 6.0 | 5.4 | 3.9 | 3.0 | 2.3 | 2.2 | $\pi$mm·mrad |
| Stripping Efficiency @ $S_B$ | – | 100 | 100 | 100 | 40 | 50 | 50 | % |
| $Q$ after $S_B$ | 1 | 8 | 14 | 29 | 53 | 77 | 90 | |
| Ions/Bunch after $S_B$ | 19.9 | 8.32 | 7.06 | 8.7 | 2.26 | 2.0 | 0.6 | $\times 10^9$ |
| Norm. emittance after $S_B$ | 8.8 | 6.1 | 5.5 | 4.1 | 3.6 | 4.0 | 2.3 | $\pi$mm·mrad |

† A Tandem Source Current of 200 $\mu$A and a Pulse Length of 110 $\mu$s were assumed.

‡ Requires source development.

## The Alternating Gradient Synchrotron

The AGS is one of the two synchrotrons build during the fifties for the acceleration of protons to 30 GeV. The other accelerator (the PS, for Proton–Synchrotron) was built about the same time in CERN for the same scope. The two rings have similar design based on the strong focussing effect that can be obtained with the principal of alternating gradient magnets. Both machines nevertheless still employ the combined function structure where the bending proper of the beam on a circular path and the focussing of the motion is provided by the same magnet. The magnetic field varies radially according to an index $n$ which changes sign from one magnet to the next and has a very large absolute value in proximity of a hundred. The main parameters of the Brookhaven AGS are shown in Table 4; whereas Fig. 8 displays the lattice function of one of the 12 superperiods.

**Table 4:** AGS Parameters

| | | |
|---|---|---|
| Circumference | 807.12 | m |
| Periodicity | 12 | |
| Betatron Tunes, Horizontal & Vertical | 8.7 | |
| Transition Energy, $\gamma_T$ | 8.5 | |
| Betatron Acceptance | 45 | $\pi$mm·mrad |
| rf Frequency, Au | 2.5–4.457 | MHz |
| Harmonic Number, $h$ | 12 | |
| Peak rf Voltage | 320 | kV |
| Bunch Length, p (0.3 eV·sec) | 3.54 | m |
| Bunch Length, Au (0.3 eV·sec) | 4.88 | m |
| Magnetic Rigidity B$\rho$ at extraction | 96.7 | T·m |
| Ejection Energy, p ($\gamma$=30.9) | 28.1 | GeV |
| Ejection Energy, Au ($\gamma$=12.2) | 10.4 | GeV/u |

One of the most interesting features of the Alternating Gradient Synchrotron is the presence of the transition energy; when the beam energy reaches that value, the time required to complete one revolution does not depend in first approximation on the particle momentum. For energies below the transition energy, particles with larger momentum advance with respect to those with lower momentum; the opposite is true for energies above the transition energy. Thus during the acceleration cycle, the beam will cross the transition energy, at which time to restore the focussing of the longitudinal motion the rf waveform is also made to jump phase. Crossing of the transition energy is a typical feature of the strong focussing and it was demonstrated successfully in both Brookhaven and CERN synchrotrons. Though, because of different charge–to–mass ratio, heavy ions can be accelerated only to 12-15 GeV/u, nevertheless crossing of the transition energy cannot be avoided also for them.

At the present beams of Silicon and Oxygen ions completely stripped are being accelerated successfully in the AGS to 15 GeV/u. The beams are then used for experiments dealing mostly for the understanding of transition of phase of high density nuclear matter. Similar experiments with somewhat larger energies, around a hundred GeV/u, have also been carried out in CERN, still with very light ions. With the Booster in operation, it will be possible to accelerate for the first time also very heavy ions completely stripped in the AGS, expanding therefore the capability to explore phenomena with even larger density in nuclear matter.

Concerning acceleration of protons, at the moment the intensity of the beam is space–charge limited at injection. With 12 bunches, at most it is possible to accelerate $1 \times 10^{13}$ protons. For a given normalized emittance and bunching factor, the maximum intensity that can be injected depends on the injection energy alone and not on the accelerator circumference. The Booster is designed to accelerate the same amount of proton intensity but on a circumference which is one fourth of the AGS circumference; this in principle should allow an increase also of a factor of four in intensity in the AGS. To accommodate for this, nevertheless the Booster has to be considerably faster and inject into the AGS at sufficiently larger energy.

On the other end, acceleration of heavy ions does not present problems with space charge. Once the beam is extracted from the Booster, the three bunches are immediately injected and accelerated into the AGS. The two rings have about the same repetition rate for this mode of operation. Since the ions are now completely stripped and their initial velocity is considerably larger, only a modest vacuum improvement is required to provide a sufficiently large survival rate against the loss for electron capture due to scattering with the residual gas. Also the acceleration proper does not seem to cause difficulties; the rf swing is now modest since at most the beam velocity ranges from $\beta = 0.7$ to about 1.

### The Transfer between and RHIC

At the end of acceleration, one beam pulse made of three bunches of heavy ions is extracted from the AGS at the rate of about one pulse per two seconds. The beam is either transported to the experimental area for immediate exploitation or transferred to the Relativistic Heavy Ion Collider. In the latter case the beam enters first a one–hundred meter long transport line. This is shown in Fig. 9; it is made of two sections. The first section follows immediately the extraction septum magnet and it is made of a sequence mostly of quadrupole magnets; at the end, a switch dipole magnet sets the beam on one of two arcs, bending in opposite direction, for injection in one of the two rings that make the RHIC. The two parts of the second section have identical magnet structure (except that, as we said, bend in opposite directions). The structure is made of combined function magnets. An important requirement of the transfer line is to preserve the beam properties like transverse emittance; to obtain this the lattice and dispersion functions are to be carefully matched at both ends.

## The Relativistic Heavy Ion Collider

The Collider is the last stage of the Heavy Ion facility of Brookhaven National Laboratory. Its construction is supposed to start in 1991 and will take about seven years for completion. It will be entirely located in a tunnel already existing on site that was meant originally for another project later cancelled.

The main goal of the RHIC is to provide head–on collision between two beams of heavy ions at relativistic energies, among other things, for the study of transition of phase of very high density matter and the formation of a new state of matter defined as a plasma of free gluons and quarks that should have existed right after the original Big Bang, the explosion that created the Universe.

There are three major requirements: first, a specific energy of at least 100 GeV/u per beam; since the two beams collide head–on, the energy available in the center–of–mass frame is twice as high, considerably larger than in the case only one beam is used on a fixed target. Second, an initial luminosity of at least $10^{27}$ cm$^{-2}$ s$^{-1}$ in the case the two beams are made of ions of gold (Au). The luminosity is a measure of the density occupied in a given region by the particles of both beams. If one is studying nuclear events which have a probability to occur given by a cross–section figure in cm$^2$, then the number of events that are produced per second is given by the product of the luminosity per the corresponding cross–section. Third, a luminosity lifetime of at least 10 hours. That is, the two beams are required to circulate and collide for that long period of time without considerably particle losses and beam size enlargement.

The main parameters of the RHIC are shown in Table 5. Since the two beams have the same sign of the electric charge and are to move in opposite direction, two magnetic rings independent from each other are required; this is shown in Fig. 10. The two rings are side–by–side in a horizontal configuration where the two beams are separated by 90 cm. The structure is divided in six arcs and an equal number of long straight sections. Each arc is made of 12 FODO cells with the lattice functions shown in Fig. 11. The insertion, shown in Fig. 12 where the two beams are brought together for collision have roughly an anti–symmetric configuration made of a sequence of 9 quadrupoles on each side of the crossing point. The amplitude value at the crossing point $\beta^*$ varies between 2 and 6 meter; the dispersion at that location is zero. The major beam and performance parameters are listed in Tables 6 and 7. Each beam is made of 57 bunches, each about one meter long and carrying $10^9$ ions of gold or $10^{11}$ protons in the other extreme.

**Table 5:** RHIC Parameters

| | | |
|---|---|---|
| Circumference | 3833.8 m | |
| Periodicity | 3 | |
| $\nu_x$ and $\nu_y$ | 28.82 | |
| Quadrupoles | 72 T/m | 1.13 m |
| Dipoles | 3.45 T | 9.46 m |
| Bending Radius | 243.24 m | |
| Transition Energy | 24.8 | |
| Phase Advance/Cell | $88.2^o$ | |
| $\beta^*$ | 2–6 m | |
| $\eta^*$ | 0 m | |
| Natural Chromaticity | -45 at | $\beta^* = 6$ m |
| | -74 | $\beta^* = 2$ m |

**Table 6:** RHIC Beam Parameters

| | Proton | | Au |
|---|---|---|---|
| No. of Bunches | 57 | | 57 |
| No. of Ions/Bunch | $10^{11}$ | | $10^9$ |
| Normalized Emittance | | | |
| Initial | 20 $\pi$mm·mrad | | 10–60 |
| After 10 hrs. | 20 | | 60–70 |
| RMS Bunch Length | | 30 cm | |
| Bunch Separation | | 220 nsec | |

The requirements of the experimental program is to provide collision among a large range of ions, from protons to Uranium, if an adequate source for this element should also exist. Not only collision between equal species like Au on Au, but also mixed cases like Au on proton are required. Table 7 summarizes the performance of the collider for different ion cases; the case of gold on gold is taken as the reference in the RHIC design because the most demanding.

Because of the large charge state of the ions, the beam dynamics and performance is dominated by IntraBeam Scattering. This is the phenomena by which two particles moving together in the same bunch scatter frequently with each other because of the Coulomb repulsive forces; during the scatter the particles exchange their momenta and, in particular, longitudinal momentum can be transferred to the transverse one and vice–versa. This has the effect to cause a continuous increase of the beam emittance and momentum spread which must be confined within the magnet aperture and contained by the available rf system. Intrabeam scattering cause also an effect on the luminosity lifetime which is required to be at least ten hours. The RHIC lattice has been chosen to minimize the effect and to fulfill the requirement.

**Table 7:** Initial Luminosity at Top Energy ($\alpha = 0$) $\beta* = 2$m

| | $N_B$ | E/A (GeV/u) | $\epsilon_N/\pi$ (mm·mrad) | Luminosity ($cm^{-2}sec^{-1}$) |
|---|---|---|---|---|
| | $\times 10^9$ | | | |
| Proton | 100 | 250.7 | 20 | $1.4 \times 10^{31}$ |
| Oxygen | 8.3 | 124.9 | 10 | $9.8 \times 10^{28}$ |
| Silicon | 5.6 | 124.9 | 10 | $4.4 \times 10^{28}$ |
| Copper | 2.7 | 114.9 | 10 | $9.5 \times 10^{27}$ |
| Iodine | 1.5 | 104.1 | 10 | $2.7 \times 10^{27}$ |
| Gold | 1.0 | 100 | 10 | $1.1 \times 10^{27}$ |
| Gold | 1.0 | 100 | 60 | $2 \times 10^{26}$ |

In the design of a heavy–ion ring an important consideration is the range of magnetic rigidity required; this range is the same for all ions including protons. In the case of RHIC at injection $B\rho = 98$ Tm and at top energy $B\rho = 840$ Tm which in the case of Au corresponds to specific kinetic energy of exactly 100 GeV/u. Since the circumference of the collider is preassigned (it must fit the present tunnel), one can determine the magnetic field required which is 3.5 Tesla. Such a field can be achieved only with superconducting magnets. Fig. 13 shows the cross–section of a regular dipole magnet which is of the $\cos\theta$ type, and Fig. 14 the cross–section of a regular quadrupole. The strength of the magnetic field is not very excessive when compared to the 4.5 Tesla reached in the Tevatron at

Fermilab and to the 6.5 Tesla required for the SSC project which is a proton–proton collider at 20 TeV per beam. The RHIC magnets have been successfully demonstrated with few prototypes; the measurements of their maximum field are shown in Fig. 15.

## Figure Captions

Figure 1. The BNL Heavy Ion Beam Facility.

Figure 2. A Closer View of the Heavy Ion Injector for RHIC.

Figure 3. The Van de Graaff High Voltage Terminal.

Figure 4. Tandem Van de Graaff with Stripping Targets.

Figure 5. Arrangement of the Two Model MP Tandem Van de Graaff Accelerators, showing alternative heavy ion beams entering transfer line to the AGS and Booster.

Figure 6. The Layout of the AGS–Booster.

Figure 7. Amplitude and Dispersion Functions for the Booster Lattice.

Figure 8. The Alternating Gradient Synchrotron.

Figure 9. Schematic Layout of the Beam Transfer Line from the AGS to RHIC.

Figure 10. Layout of the Collider.

Figure 11. A RHIC FODO Cell.

Figure 12. Expanded Layout of Half–Insertion.

Figure 13. Cross–Section of the RHIC Dipole Magnet.

Figure 14. Cross–Section of the RHIC Quadrupole Magnet.

Figure 15. Training History of Dipoles DRA001–004.

Figure 1.

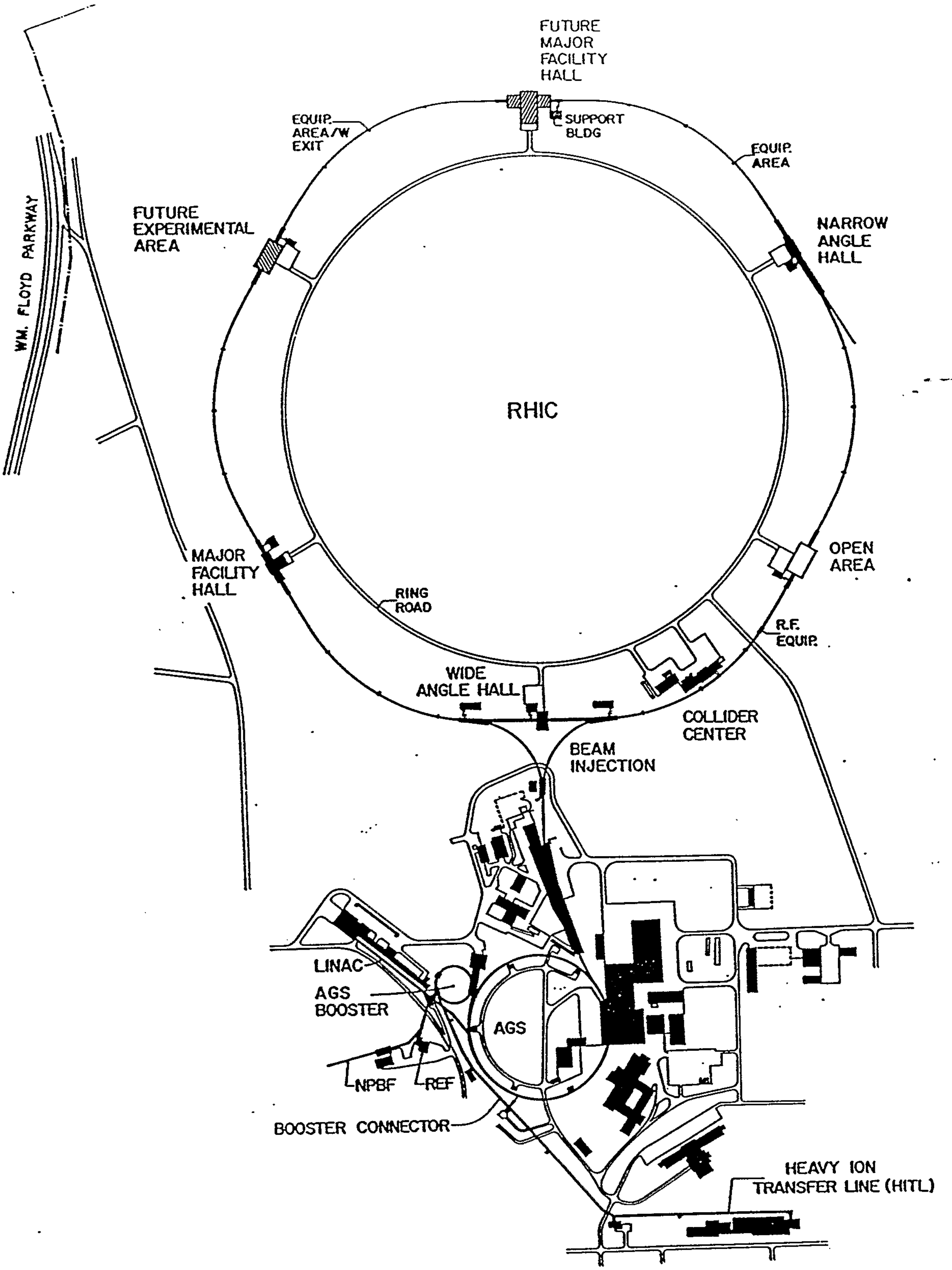
FUTURE
MAJOR
FACILITY
HALL
SUPPORT
BLDG
EQUIP.
AREA/W
EXIT
EQUIP.
AREA
FUTURE
EXPERIMENTAL
AREA
NARROW
ANGLE
HALL
WM. FLOYD PARKWAY
RHIC
MAJOR
FACILITY
HALL
OPEN
AREA
RING
ROAD
R.F.
EQUIP.
WIDE
ANGLE HALL
COLLIDER
CENTER
BEAM
INJECTION
LINAC
AGS
BOOSTER
AGS
NPBF
REF
BOOSTER CONNECTOR
HEAVY ION
TRANSFER LINE (HITL)

Figure 2.

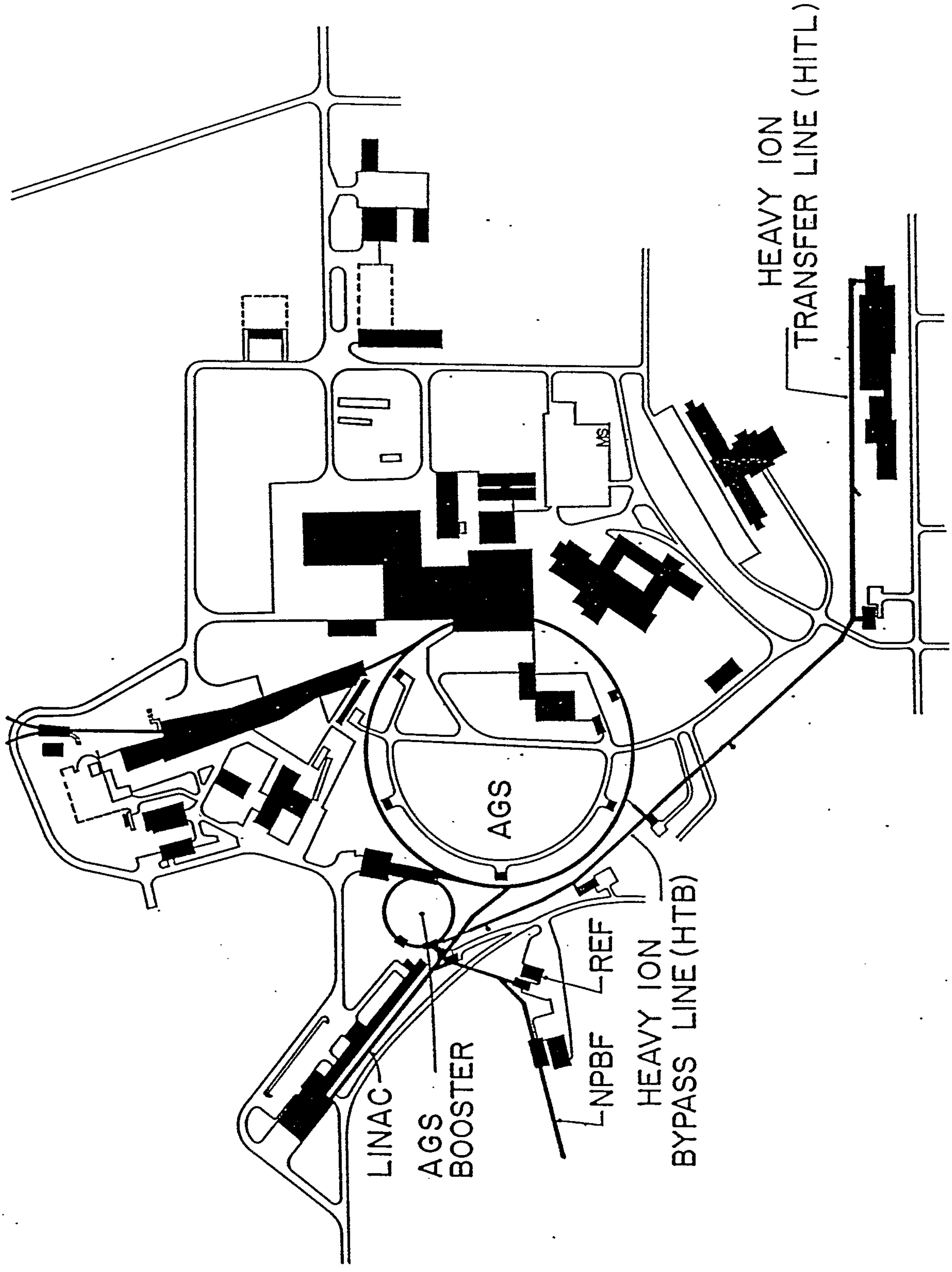

HEAVY ION
TRANSFER LINE (HITL)
AGS
LINAC
AGS
BOOSTER
NPBF
HEAVY ION
BYPASS LINE (HTB)
REF

Figure 3.

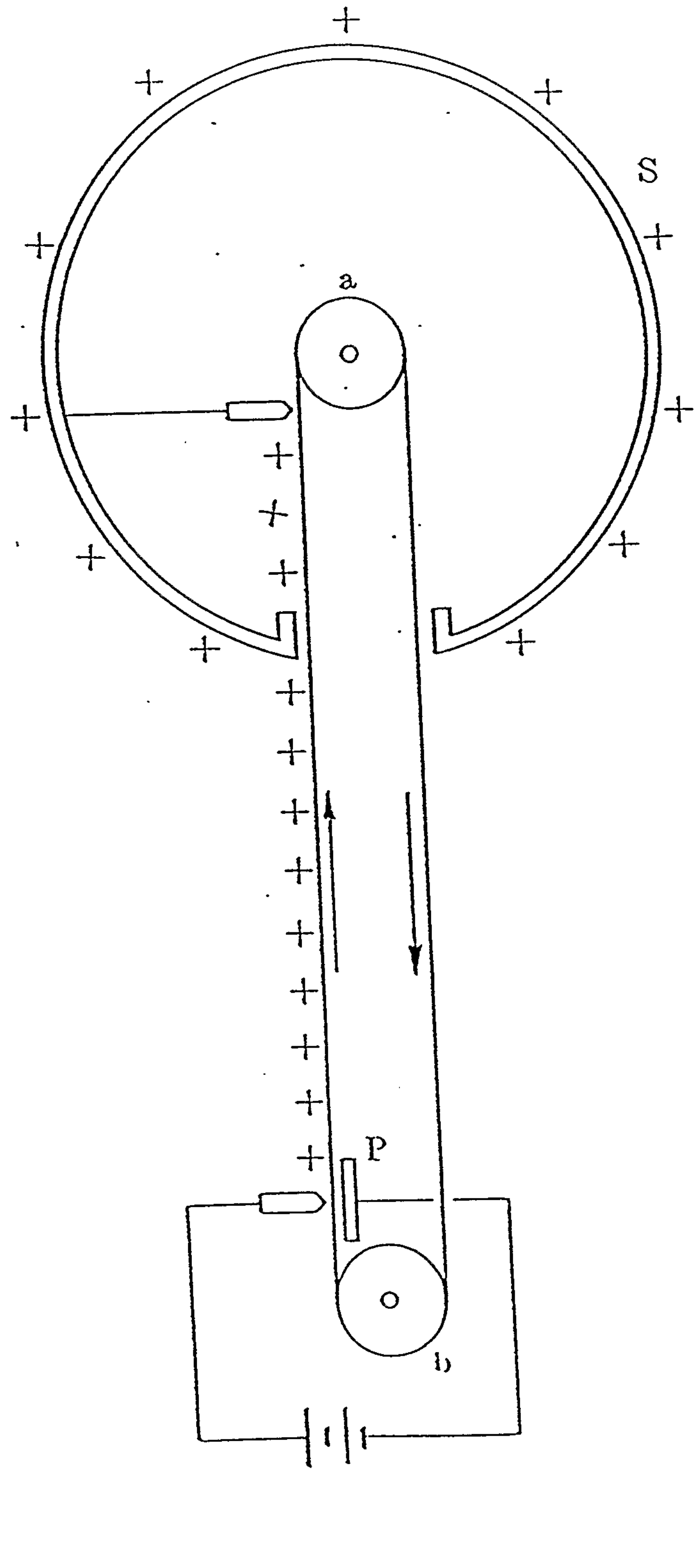

Figure 4.

TANDEM VAN DE GRAAFF

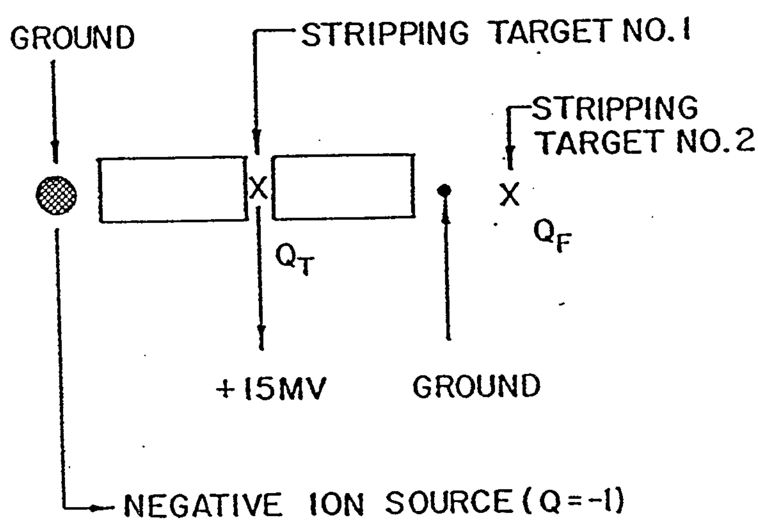


FINAL KINETIC ENERGY (TWO-STAGE MODE)

$$= 15\,\text{MeV} + Q_T \cdot 15\,\text{MeV}$$

Figure 5.

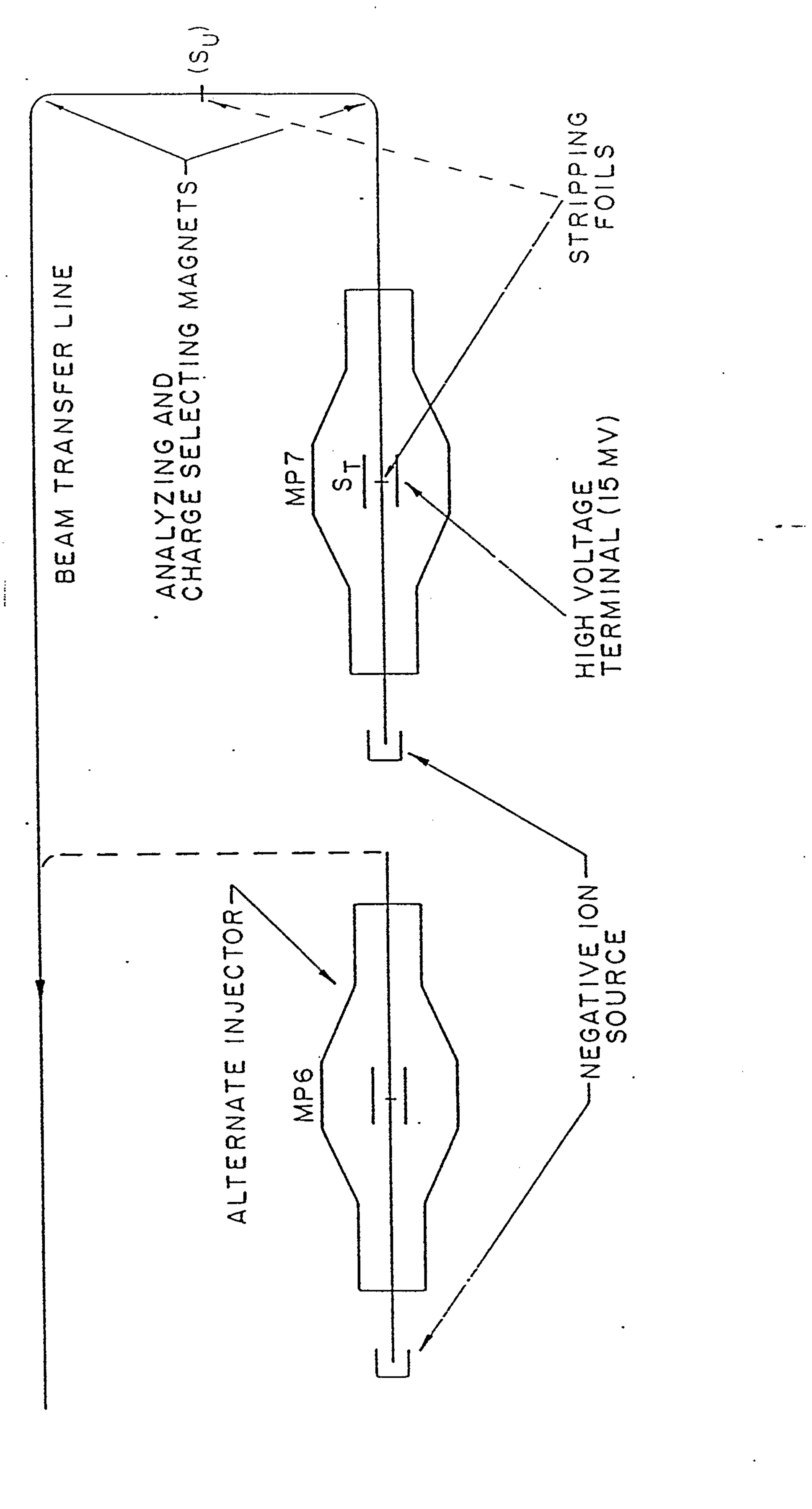

(S_U)
BEAM TRANSFER LINE
ANALYZING AND
CHARGE SELECTING MAGNETS
STRIPPING
FOILS
MP7
S_T
HIGH VOLTAGE
TERMINAL (15 MV)
NEGATIVE ION
SOURCE
ALTERNATE INJECTOR
MP6

Figure 6.

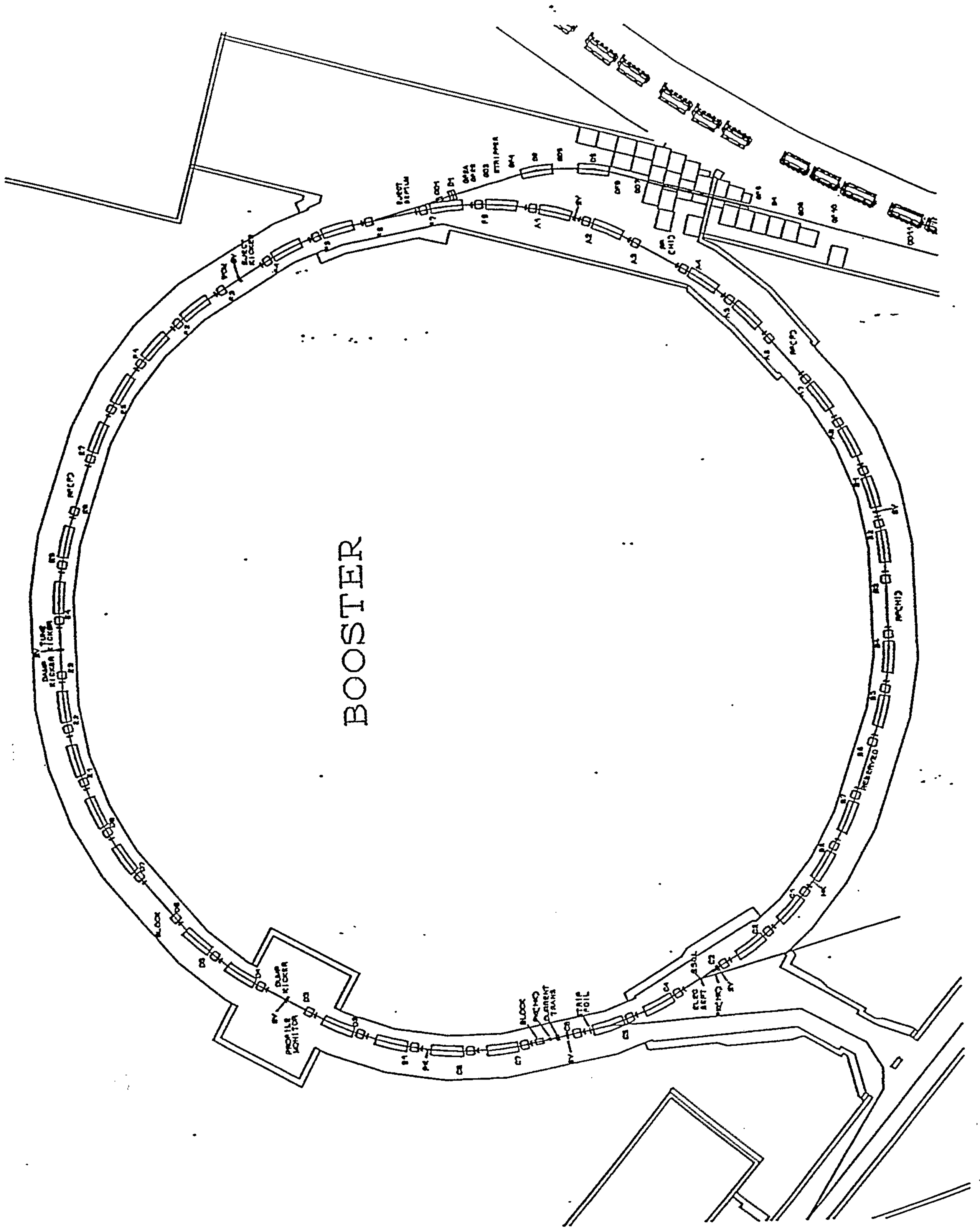

Figure 7.

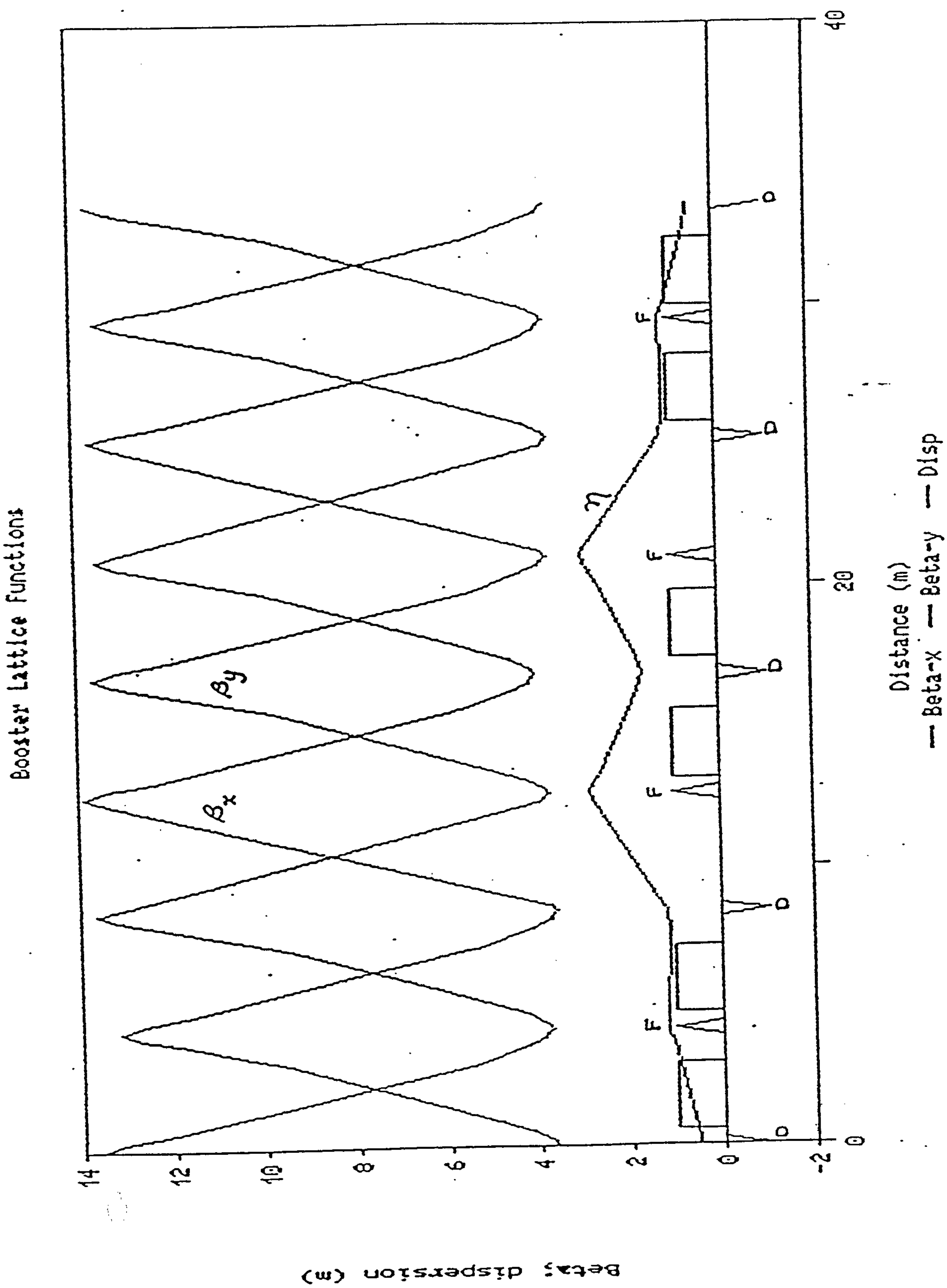

Booster Lattice Functions
Beta; dispersion (m)
Distance (m)
— Beta-x — Beta-y — Disp
$\beta_x$
$\beta_y$
$\eta$
F
D
14
12
10
8
6
4
2
0
-2
0
20
40

Figure 8.

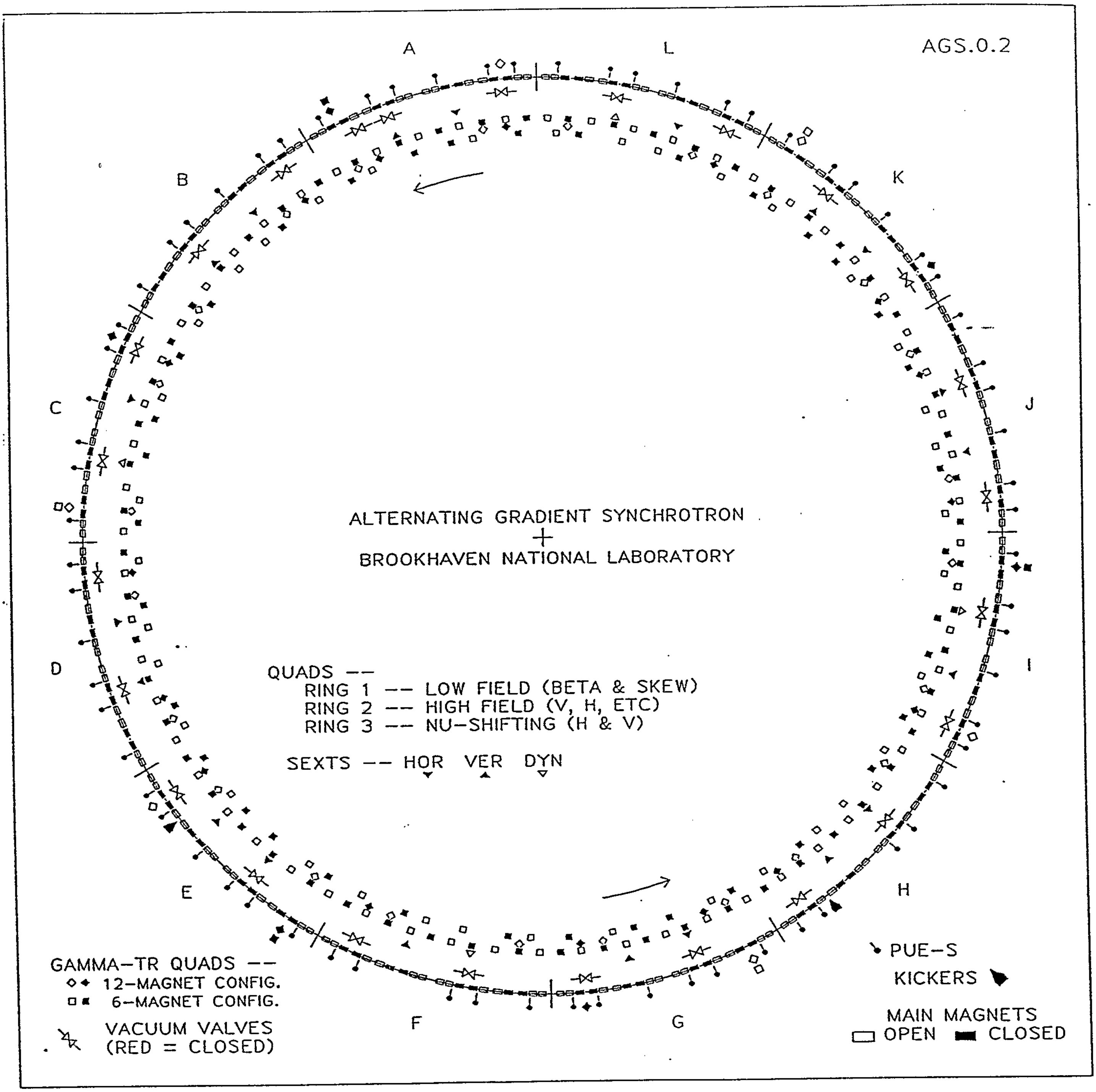
AGS.0.2
A
L
K
J
I
H
G
F
E
D
C
B
ALTERNATING GRADIENT SYNCHROTRON
BROOKHAVEN NATIONAL LABORATORY
QUADS --
RING 1 -- LOW FIELD (BETA & SKEW)
RING 2 -- HIGH FIELD (V, H, ETC)
RING 3 -- NU-SHIFTING (H & V)
SEXTS -- HOR VER DYN
GAMMA-TR QUADS --
12-MAGNET CONFIG.
6-MAGNET CONFIG.
VACUUM VALVES
(RED = CLOSED)
PUE-S
KICKERS
MAIN MAGNETS
OPEN CLOSED

Figure 9.

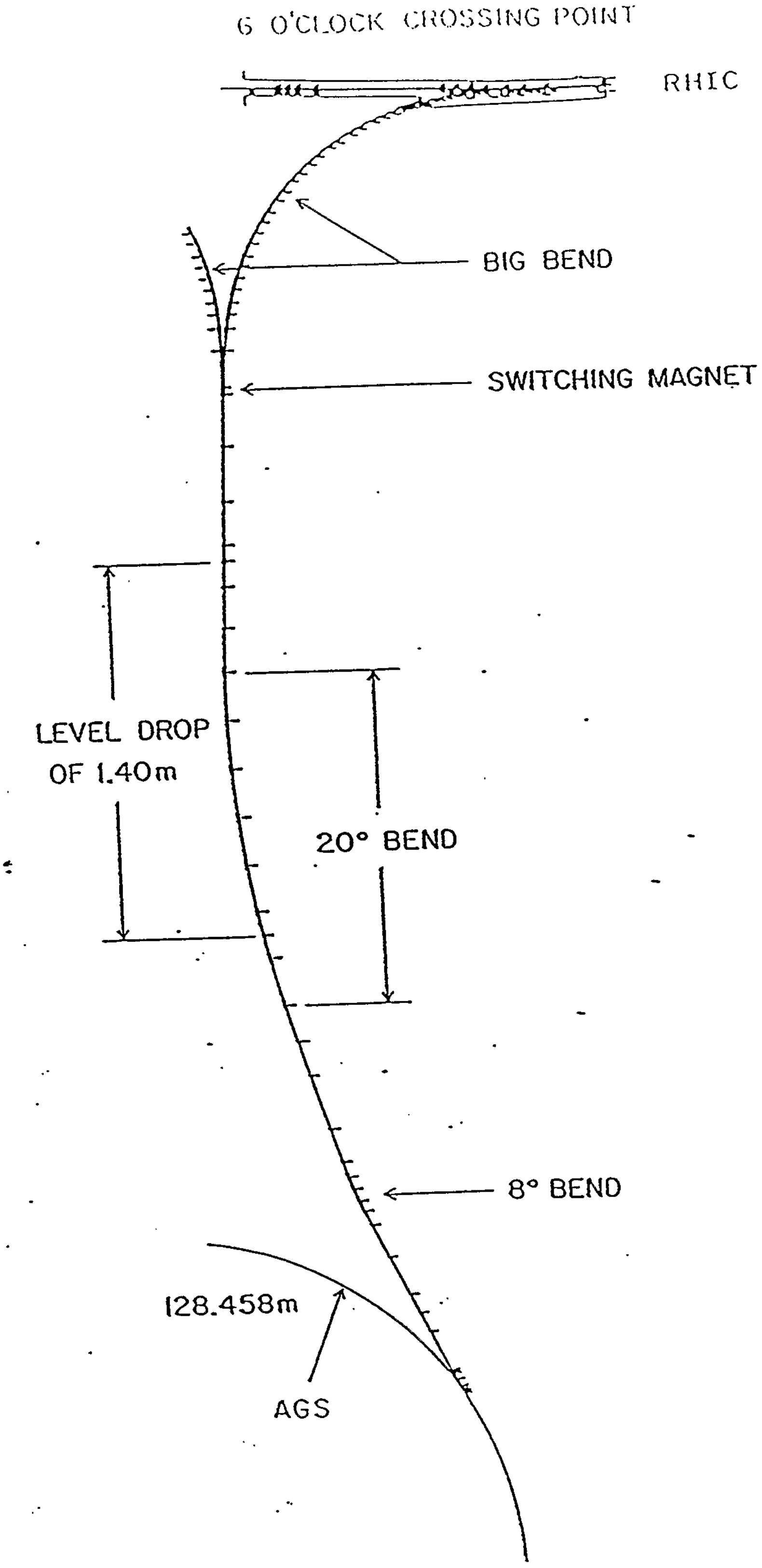
6 O'CLOCK CROSSING POINT
RHIC
BIG BEND
SWITCHING MAGNET
LEVEL DROP
OF 1.40m
20° BEND
8° BEND
128.458m
AGS

Figure 10.

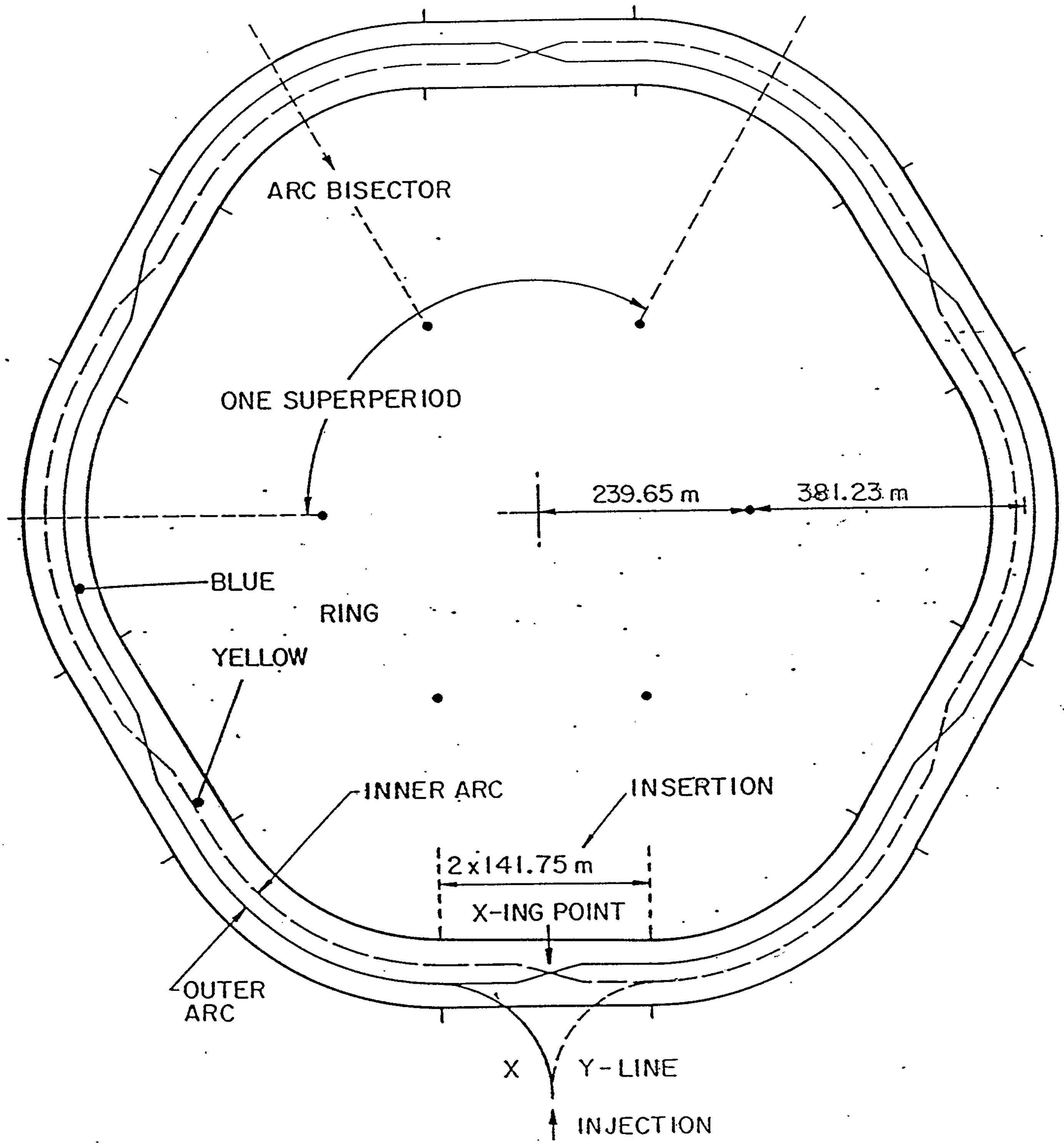

ARC BISECTOR
ONE SUPERPERIOD
239.65 m
381.23 m
BLUE
RING
YELLOW
INNER ARC
INSERTION
2 x 141.75 m
X-ING POINT
OUTER
ARC
X
Y-LINE
INJECTION

Figure 11.

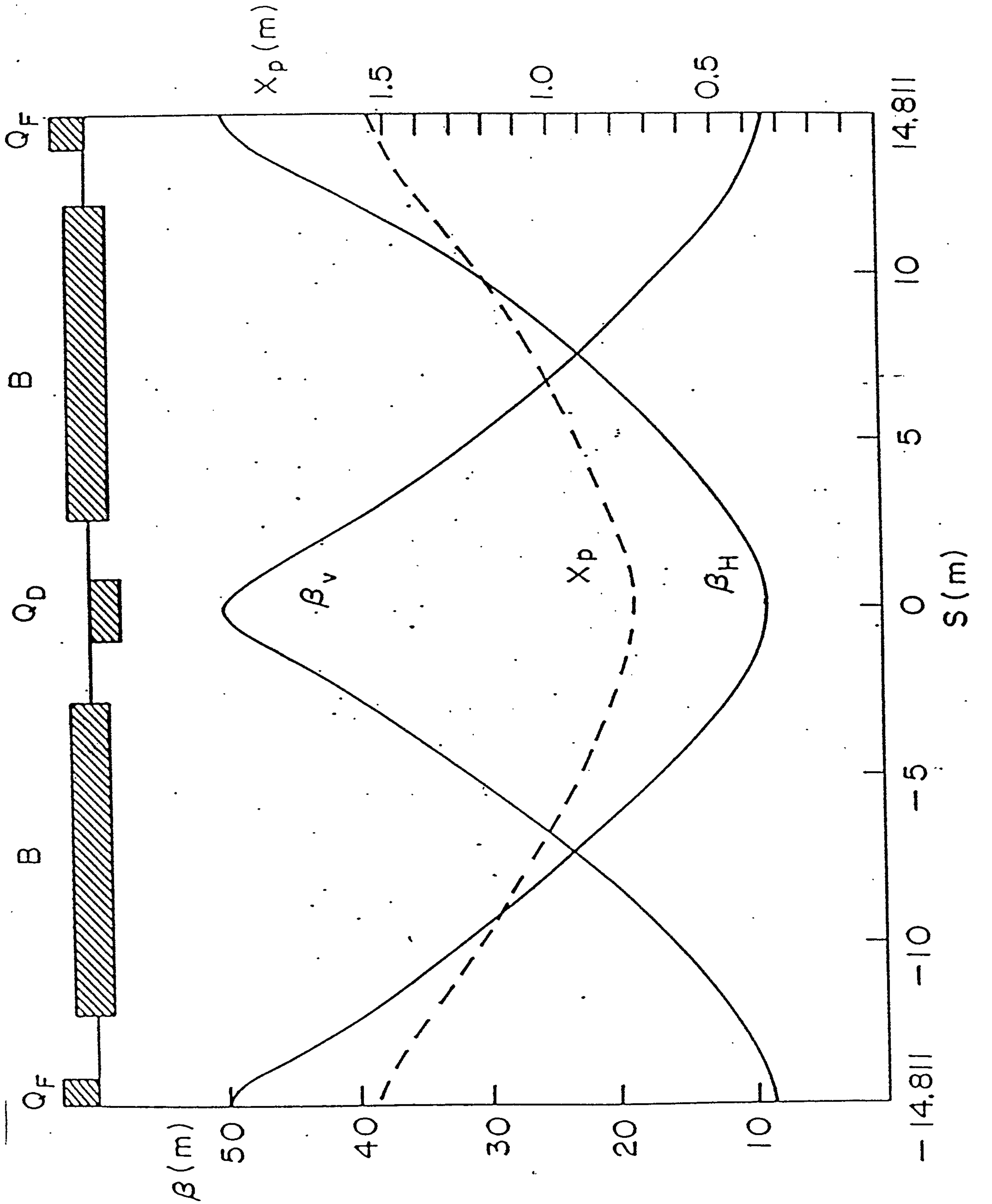

Q_F
B
Q_D
B
Q_F
β (m)
50
40
30
20
10
X_p (m)
1.5
1.0
0.5
β_V
X_p
β_H
−14.811
−10
−5
0
5
10
14.811
S (m)

Figure 12.

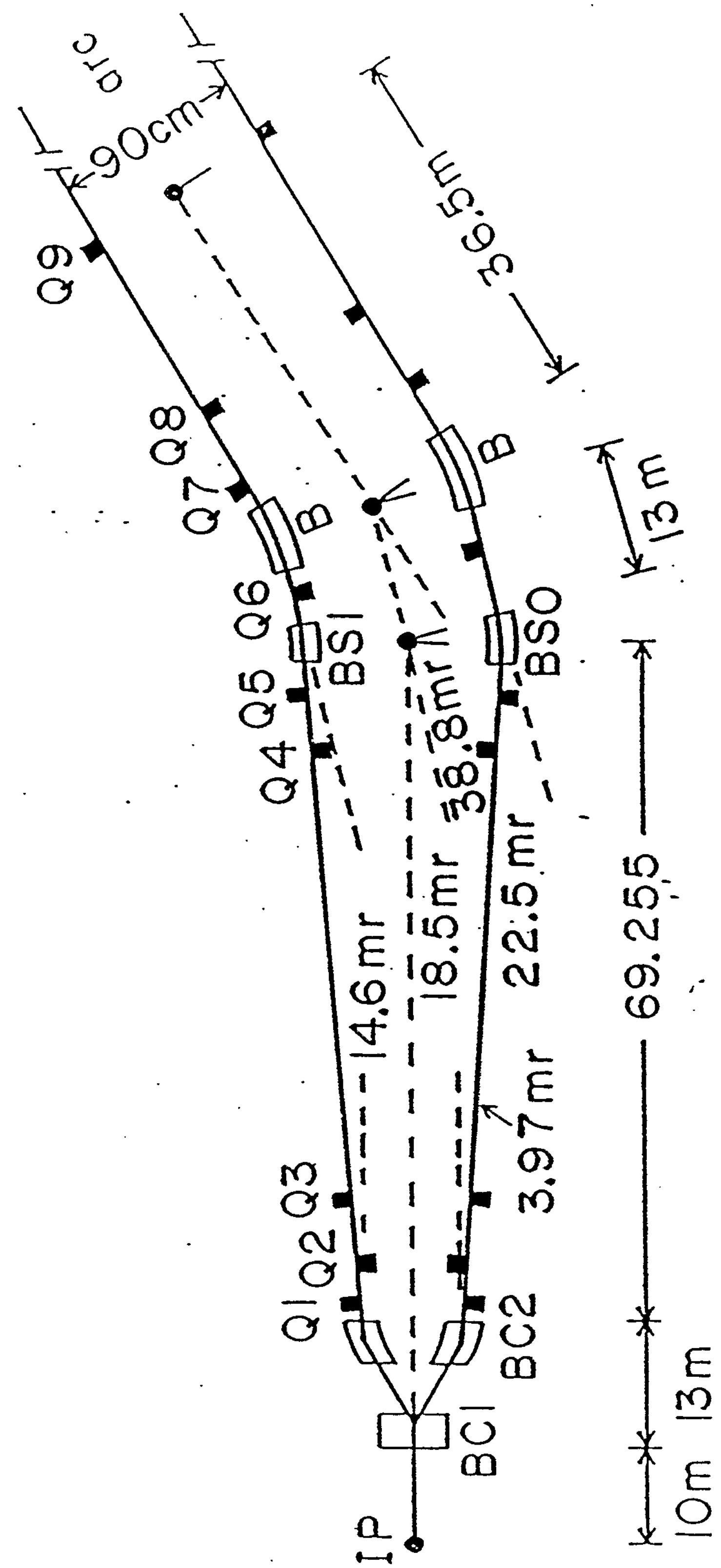

arc
90cm
36.5m
Q9
Q8
Q7
B
B
13m
Q6
BSI
Q5
BSO
Q4
38.8mr
22.5mr
69.255
14.6mr
18.5mr
3.97mr
Q3
Q2
Q1
BC2
BC1
13m
10m
IP

Figure 13.

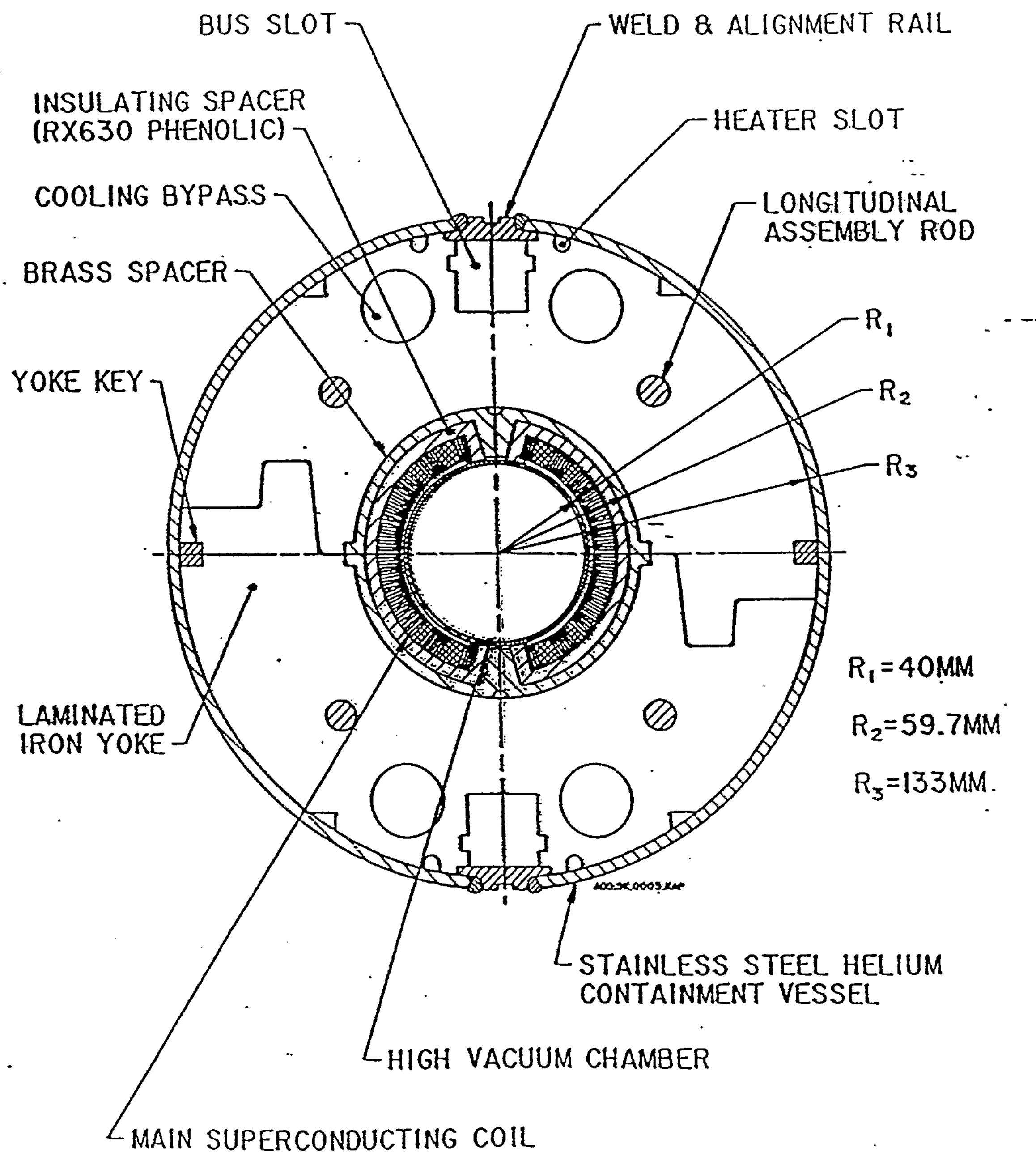
BUS SLOT
WELD & ALIGNMENT RAIL
INSULATING SPACER
(RX630 PHENOLIC)
HEATER SLOT
COOLING BYPASS
LONGITUDINAL
ASSEMBLY ROD
BRASS SPACER
$R_1$
YOKE KEY
$R_2$
$R_3$
LAMINATED
IRON YOKE
$R_1$=40MM
$R_2$=59.7MM
$R_3$=133MM.
STAINLESS STEEL HELIUM
CONTAINMENT VESSEL
HIGH VACUUM CHAMBER
MAIN SUPERCONDUCTING COIL

Figure 14.

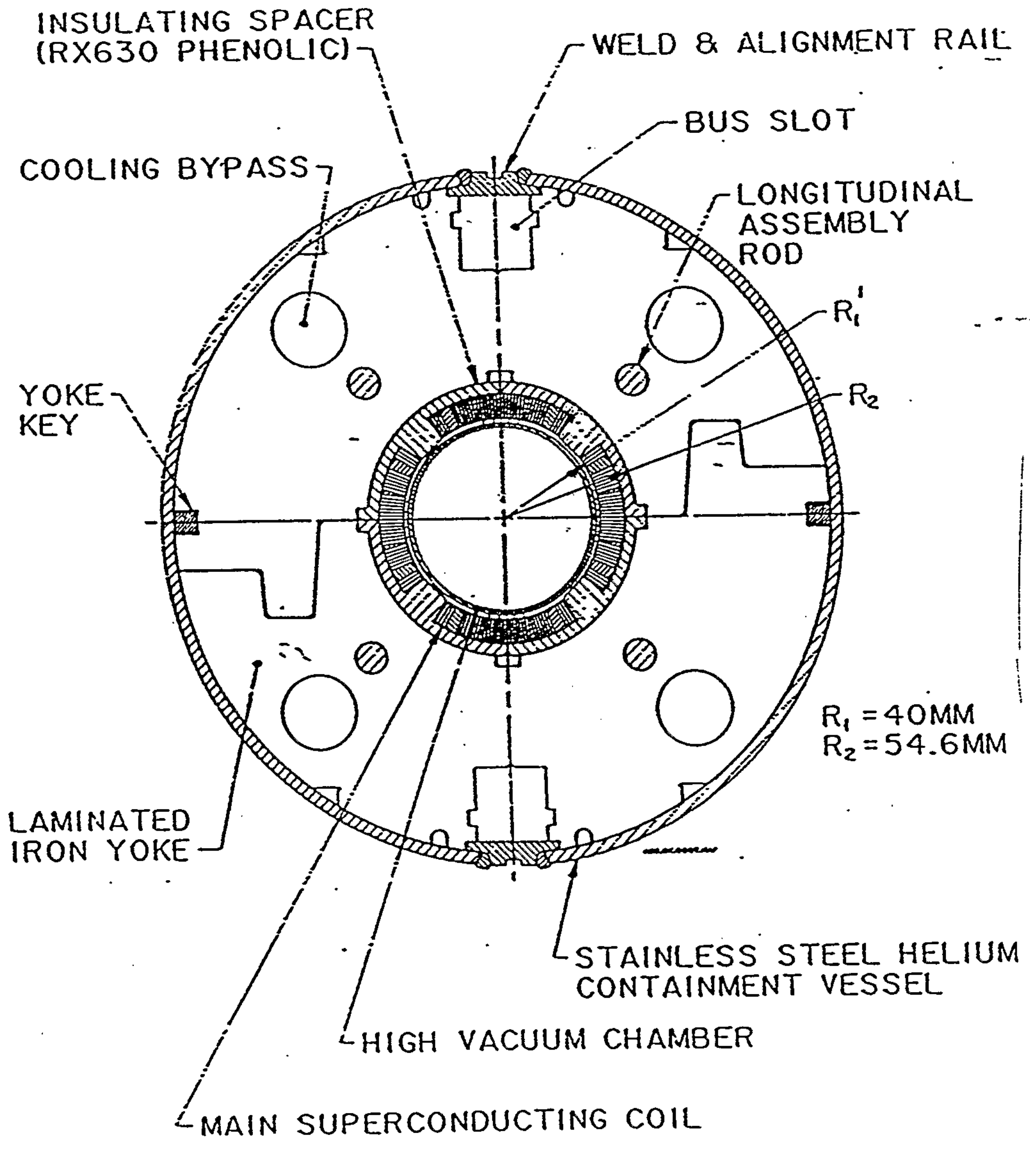
INSULATING SPACER
(RX630 PHENOLIC)
WELD & ALIGNMENT RAIL
BUS SLOT
COOLING BYPASS
LONGITUDINAL
ASSEMBLY
ROD
R1'
YOKE
KEY
R2
R1 =40MM
R2=54.6MM
LAMINATED
IRON YOKE
STAINLESS STEEL HELIUM
CONTAINMENT VESSEL
HIGH VACUUM CHAMBER
MAIN SUPERCONDUCTING COIL

Figure 15

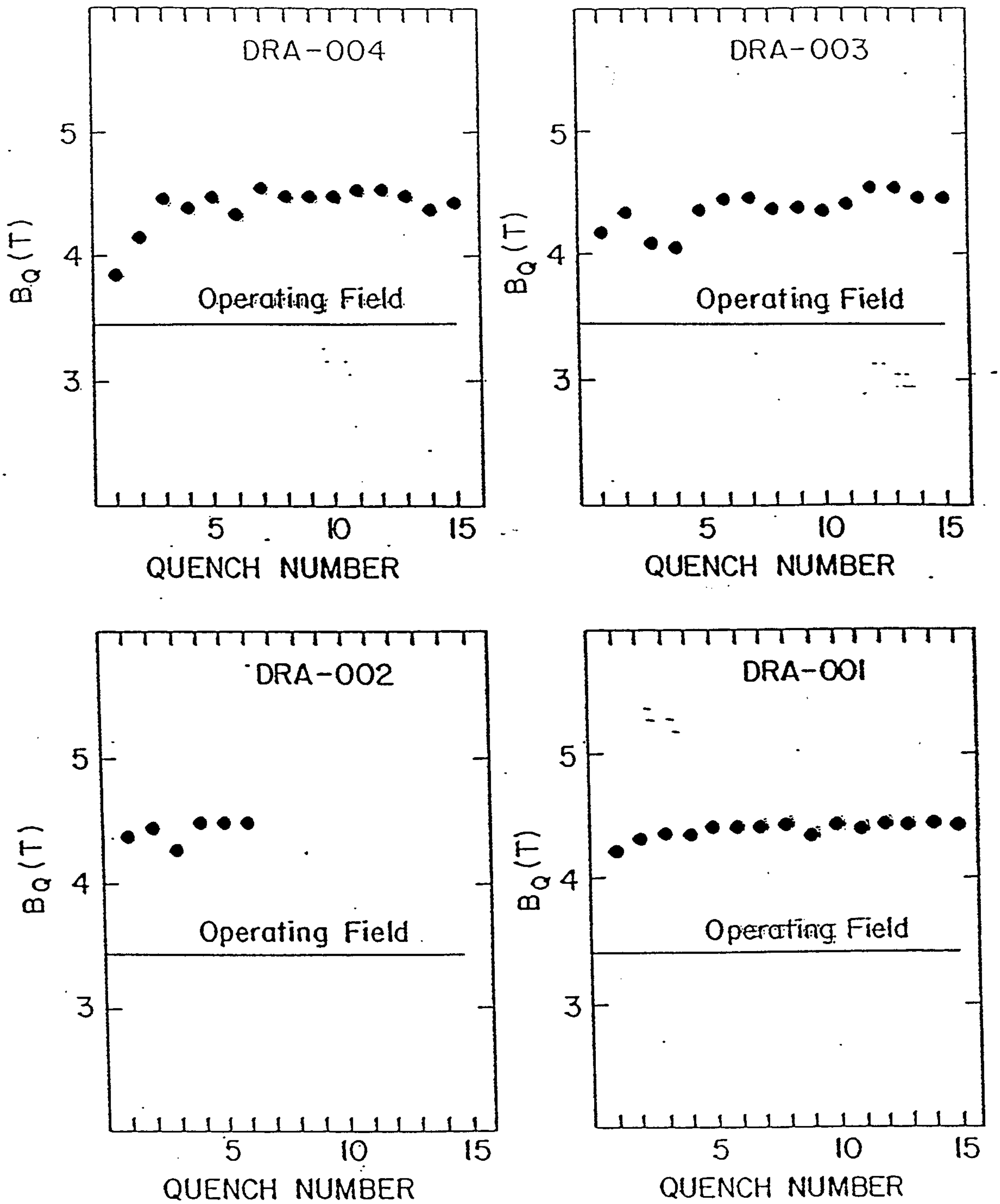

DRA-004
DRA-003
DRA-002
DRA-001
$B_Q$ (T)
Operating Field
QUENCH NUMBER
5
10
15
3
4
5